Preparation and Complexation of Polydentate and Macrocyclic Ligands incorporating Benzimidazole. *X*-Ray Crystal Structure of 6,7,9,10,12,13,15,16-Octahydro-23*H*,25*H*-bis(benzimidazo[1,2-*j*:2′,1′-*o*])[1,4,7,13,10,16]tetraoxa-diazacyclo-octadecine†

William Clegg, Joyce C. Lockhart,* and Faleh H. Musa
Department of Inorganic Chemistry, The University, Newcastle upon Tyne NE1 7RU

A number of ligands, including some macrocycles, all with benzimidazole units incorporated, have been synthesised. These co-ordinate Cu^{II} and other transition metals with the imidazole nitrogen and other donor atoms included in the ligand design. The crystal structure data for a representative macrocycle, 6,7,9,10,12,13,15,16-octahydro-23*H*,25*H*-bis(benzimidazo[1,2-*j*:2′,1′-*o*])-[1,4,7,13,10,16]tetraoxadiazacyclo-octadecine, are presented, together with spectroscopic and other details of representative complexes.

The attention of inorganic chemists has been caught by the extraordinary complexity of the co-ordination chemistry of metals in biological systems.[1] Where the metal is incorporated in a haem, corrin or chlorin ring, or an Fe–S cluster, it has been possible by extrusion of the metal-containing entity as a small manageable moiety, to define its co-ordination. Such techniques are not applicable to copper-containing metalloproteins, where the copper-binding sites are amino-acid side chains.[2] For a number of small copper proteins, crystal-structure determination at high resolution has defined the environment of copper, *e.g.* in Type 1 proteins Cu is ligated by two histidine nitrogens and cysteine and methionine sulphur.[3] The geometry has the distorted tetrahedral square-planar arrangement which is a recognisable feature of nature's design for rapid electron transport *via* Cu.[2,3] Histidine is also involved in copper co-ordination in many other copper proteins such as cytochrome oxidase, superoxide dismutase, and haemocyanin.[2] The challenge of synthesising model ligands which will provide a sequence of ligand donor atoms similar to those in the binding site of the copper proteins has been taken up and many new ligands have been produced for this purpose. Thus it is of interest to produce multidentate ligands containing the requisite imidazole, oxy, and thio residues which appear to be in the copper co-ordination spheres,[2] to add to the growing list[4–15] of model ligands for the copper sites in these extremely important proteins. We have employed syntheses which link two benzimidazole units at the 2-position,[16,17] and we have used the secondary nitrogen function of the resultant benzimidazoles, *e.g.* L^1, to form macrocycles and polydentate ligands with other donor links in the chain, *e.g.* L^6. Several ligands with imidazole and additional thioether or amino donor groups have been synthesised recently.[4–14] Of the open-chain ligands L^1—L^5, only L^4 has been reported[10] in copper complexes when we began this work, but complexes of ligands L^1 and L^3 have since been reported.[4] This paper completes a set of ligands L^2—L^5 now available with either O- or S-donor atoms in the chain linking the benzimidazoles. Ligands L^6—L^{11} are the first macrocyclic examples; modelling studies suggest these ligands should have a tri- or tetra-dentate function which could co-ordinate copper *exo* to the macrocyclic ring. The possible alkali-co-ordinating function of the macrocyclic ether ring was explored. Future work will explore the potential of dimeric forms of the macrocycles as binucleating ligands.

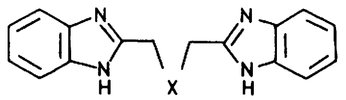

	X
L^1	O
L^2	OCH_2CH_2O
L^3	S
L^4	CH_2SCH_2
L^5	OC_6H_4O

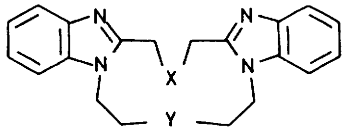

	X	Y
L^6	O	OCH_2CH_2O
L^7	O	$O(CH_2CH_2O)_2$
L^8	OC_6H_4O	O
L^9	OCH_2CH_2O	$O(CH_2CH_2O)_2$
L^{10}	CH_2SCH_2	$O(CH_2CH_2O)_2$
L^{11}	CH_2SCH_2	OCH_2CH_2O

Copper(II) complexes of tri- and tetra-dentate ligands, where there are one or two thioether donor groups in addition to the benzimidazole nitrogens, exhibit several modes of co-ordination. These are shown in Figure 1. The tetradentate NSSN ligands can adopt the trigonal bipyramidal co-ordination[6–8] shown in Figure 1(*a*), in which *X*-ray crystal data show a Cu–S distance of *ca.* 2.4—2.9 Å (*cf.* Type 1[3] copper–methionine interaction). Tridentate NSN ligands were found in distorted trigonal-bipyramidal co-ordination [Figure 1(*b*)], but also in square-based pyramidal[10] co-ordination, and in one case, linear co-ordination.[5] Octahedral [Figure 1(*c*)] and trigonal-bipyramidal co-ordination have been found for imidazole ligands with NSSN[9] donors. Tridentate NSN and the corresponding N(NH)N ligands[4] also gave 2:1 ligand–metal complexes which were octahedral [Figure 1(*d*)]. The N(NH)N

---

† *Supplementary data available* (No. SUP 56358, 7 pp.): H-atom co-ordinates, thermal parameters, packing diagram of L^7, views of L^7 perpendicular to benzimidazole plane and showing parallel planes of benzimidazole moieties. See Instructions for Authors, *J. Chem. Soc., Dalton Trans.*, 1986, Issue 1, pp. xvii–xx. Structure factors are available from the editorial office.

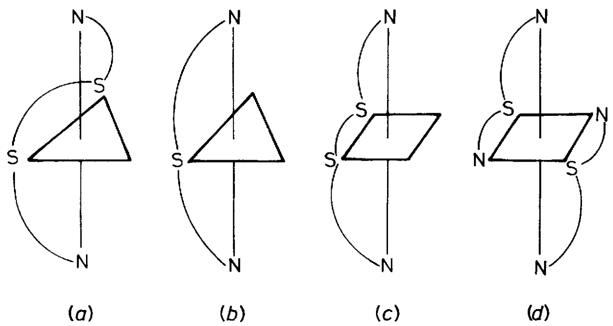

Figure 1. Observed geometries for NSN and NSSN ligands

type ligand has been observed in an octahedral 1:1 complex.[12] The new complexes described in this paper are compared with established structures.

Experimental

The bisbenzimidazoles L^1—L^5 were prepared by literature methods[16,17] from the corresponding carboxylic acids. New ligands were characterised as indicated in Table 1. Some were converted further into macrocycles as follows.

Preparation of L^7.[*]—To a stirred suspension of NaH (1.5 g obtained from an 80% suspension in oil, 0.063 mol) in freshly distilled tetrahydrofuran (125 cm^3) under N$_2$, an equimolar mixture of 1,3-bis(benzimidazol-2-yl)-2-oxapropane (2.78 g, 0.01 mol) plus 1,11-bis(*p*-tolylsulphonyloxy)-3,6,9-trioxaundecane (4.74 g, 0.01 mol) in dimethyl sulphoxide (30 cm^3) was added dropwise over 30—40 min. The mixture was refluxed for 24 h. After filtration the residual solution was diluted with water to give a precipitate of L^7 (yield = 1.0 g, 23%), which was recrystallised from ethanol to give colourless crystals.

By a similar route, the macrocycles L^6 and L^8 were prepared. Characterising data are shown in Table 1.

Preparation of L^9.[†]—In a similar technique, L^2 (3.22 g, 0.01 mol) was reacted in tetrahydrofuran (100 cm^3) with sodium hydride (0.7 g, 0.03 mol), and then with 1,11-bis(*p*-tolylsulphonyloxy)-3,6,9-trioxaundecane (5.02 g, 0.01 mol), giving a thick red oil. The separation differed from that described for L^7. The red oil was purified by the Celite technique using a Fluorosil column; L^9 was eluted with a mixture of diethyl ether–chloroform–acetone (70:20:10) as a very thick pale yellow oil. This on recrystallisation from ethanol gave thick waxy needles, m.p. 40 °C. On grinding, and after a day under vacuum, these melted at 110 °C.

Macrocycles L^{10} and L^{11} were obtained by a similar technique as colourless solids which, dried under vacuum, melted at 167 and 255 °C respectively. See Table 1 for analytical details. From later fractions of the chromatographic separation of L^{11} a compound L^{11a} [m.p. 158 °C (acetone)] was obtained, which analysed for the same empirical formula as L^{11}, but which had a mass spectrum indicating an oligomer; there was no parent ion. Absorption coefficients in the u.v. spectrum were worked out (Table 5) on the basis of the monomer molecular weight and are consistent with a simple oligomer. The compound L^{11a} was insufficiently soluble for n.m.r. investigation.

Table 1. Analytical data for polydentate benzimidazoles[a]

Ligand	Formula	M.p./°C	Analysis[b] (%) C	H	N	Accurate mass[b,c]
L^2	C$_{18}$H$_{18}$N$_4$O$_2$	258	67.1	5.7	17.1	322.1446
			(67.1)	(5.6)	(17.4)	(322.1430)
L^6	C$_{22}$H$_{24}$N$_4$O$_3$	198	67.6	6.1	14.2	392.1855
			(67.3)	(6.2)	(14.3)	(392.1848)
L^7	C$_{24}$H$_{28}$N$_4$O$_4$	174	65.7	6.3	12.7	436.2112
			(66.0)	(6.5)	(12.8)	(436.2110)
L^8	C$_{26}$H$_{24}$N$_4$O$_3$	258	70.6	5.2	12.6	440.1843
			(70.9)	(5.5)	(12.7)	(440.1848)
L^9	C$_{26}$H$_{32}$N$_4$O$_5$	110	65.3	6.6	11.6	480.2385
			(65.0)	(6.7)	(11.7)	(480.2374)
L^{10}	C$_{26}$H$_{32}$N$_4$O$_3$S[d]	167	65.6	6.8	11.4	480.2176
			(65.0)	(6.7)	(11.7)	(480.2195)
L^{11}	C$_{24}$H$_{28}$N$_4$O$_2$S[e]	255	65.0	6.4	12.6	*m/e* 436
			(66.1)	(6.4)	(12.8)	(436.1901)
L^{11a}	C$_{24}$H$_{28}$N$_4$O$_2$S	158	65.3	6.4	12.6	

[a] Characteristic i.r. absorptions observed (cm^{-1}): L^1—L^5 1 625, 1 580; L^6—L^{11} 1 612—1 610 cm^{-1}. [b] Required values in parentheses. [c] Measured on an AEI MS9 mass spectrometer. [d] S = 7.0 (6.7)%. [e] S = 7.8 (7.4)%.

Crystal Data for L^7.—C$_{24}$H$_{28}$N$_4$O$_4$, M = 436.5, orthorhombic, a = 25.138(2), b = 5.179 4(3), c = 16.565(2) Å, U = 2 156.8 Å^3 (by least-squares refinement on 2θ angles for 29 reflections, λ = 0.710 69 Å), space group $Pca2_1$, Z = 4, D_c = 1.344 g cm^{-3}, $F(000)$ = 928. Colourless crystal, 0.31 × 0.46 × 0.54 mm, $\mu(\text{Mo-}K_\alpha)$ = 0.87 cm^{-1}.

Data Collection and Processing.—Stoe-Siemens AED diffractometer, ω/θ scan mode, graphite-monochromatised Mo-K_α radiation, on-line profile fitting.[18] 3 782 Unique reflections ($2\theta < 50°$, h, $k \geqslant 0$, no sign restriction on l), 3 523 with $F > 4\sigma(F)$. No significant variation in intensity for three standard reflections, no absorption correction.

Structure Solution and Refinement.[19]—Multisolution direct methods, blocked-cascade refinement on F, with all non-hydrogen atoms anisotropic, hydrogens in calculated positions with C–H = 0.96 Å, U(H) = 1.2U_{eq}(C). Weighting scheme $w^{-1} = \sigma^2(F) + 0.000\,33F^2$, extinction $x = 3.4(4) \times 10^{-6}$ [$F_c' = F_c/(1 + xF_c^2/\sin 2\theta)^{\frac{1}{4}}$]. Final R = 0.032, R' [= $(\Sigma w\Delta^2/\Sigma wF_o^2)^{\frac{1}{2}}$] = 0.035. Attempt to define direction of polar c axis gave indeterminate η = 3.9(16).[20] Slope of normal probability plot = 1.38, largest peak in final difference synthesis = 0.36 e Å^{-3}, largest hole −0.20 e Å^{-3}. Scattering factors from ref. 21.

Atomic co-ordinates are shown in Table 2, important geometrical parameters in Table 3.

Metal(II) *Complexes of Bisbenzimidazoles.*—The 1:1 complexes were prepared from equimolar amounts of salt and ligand. A mixture of each dissolved in the minimum amount of ethanol sometimes gave a precipitate immediately on mixing, but usually it was necessary to reflux the mixture for 30 min. Appropriate mol ratios of salt and ligand were reacted to produce other stoicheiometries. Analytical data are shown in Table 4.

Spectroscopic Studies.—U.v. and visible solution spectra were recorded in ethanol and dimethyl sulphoxide mostly with a Perkin-Elmer 550S instrument. Near-i.r. studies were made with a Unicam SP700 spectrometer. Data on free ligands and metal complexes in the u.v. region are shown in Table 5. Solid-state

---

[*] 6,7,9,10,12,13,15,16-Octahydro-23*H*,25*H*-bis(benzimidazo-[1,2-*j*: 2′,1′-*o*])[1,4,7,13,10,16]tetraoxadiazacyclo-octadecine.

[†] 6,7,9,10,12,13,15,16,25,26-Decahydro-23*H*,28*H*-bis(benzimidazo-[1,2-*j*: 2′,1′-*r*])[1,4,7,13,16,10,19]pentaoxadiazacyclohenicosine.

Table 2. Atomic co-ordinates (× 10^4) for L^7

Atom	*x*	*y*	*z*
O(1)	5 104(1)	4 682(2)	4 125(1)
C(2)	4 694(1)	4 688(4)	3 534(1)
C(3)	4 239(1)	6 436(3)	3 737(1)
N(4)	4 063(1)	8 249(3)	3 261(1)
C(5)	3 620(1)	9 269(3)	3 659(1)
C(6)	3 279(1)	11 269(4)	3 442(1)
C(7)	2 868(1)	11 885(4)	3 950(1)
C(8)	2 788(1)	10 533(3)	4 674(1)
C(9)	3 122(1)	8 564(3)	4 909(1)
C(10)	3 545(1)	7 983(3)	4 391(1)
N(11)	3 947(1)	6 180(3)	4 436(1)
C(12)	4 048(1)	4 434(3)	5 111(1)
C(13)	4 203(1)	5 859(4)	5 877(1)
O(14)	4 646(1)	7 460(2)	5 727(1)
C(15)	4 829(1)	8 691(4)	6 441(1)
C(16)	5 248(1)	10 631(4)	6 239(1)
O(17)	5 711(1)	9 562(3)	5 875(1)
C(18)	6 059(1)	8 294(4)	6 413(1)
C(19)	6 236(1)	5 786(4)	6 083(1)
O(20)	6 559(1)	6 173(2)	5 388(1)
C(21)	6 705(1)	3 807(4)	5 012(1)
C(22)	6 303(1)	2 828(3)	4 399(1)
N(23)	6 267(1)	4 531(3)	3 695(1)
C(24)	6 638(1)	4 661(3)	3 081(1)
C(25)	7 086(1)	3 160(4)	2 913(1)
C(26)	7 377(1)	3 857(4)	2 242(1)
C(27)	7 234(1)	5 936(4)	1 762(1)
C(28)	6 786(1)	7 388(4)	1 925(1)
C(29)	6 480(1)	6 715(3)	2 597(1)
N(30)	6 011(1)	7 808(3)	2 896(1)
C(31)	5 904(1)	6 457(3)	3 549(1)
C(32)	5 439(1)	6 914(4)	4 089(1)

Table 3. Bond lengths (Å) and angles (°) for L^7

O(1)–C(2)	1.422(2)	O(1)–C(32)	1.431(2)
C(2)–C(3)	1.497(2)	C(3)–N(4)	1.304(2)
C(3)–N(11)	1.376(2)	N(4)–C(5)	1.396(2)
C(5)–C(6)	1.393(3)	C(5)–C(10)	1.396(2)
C(6)–C(7)	1.368(3)	C(7)–C(8)	1.404(3)
C(8)–C(9)	1.377(2)	C(9)–C(10)	1.401(2)
C(10)–N(11)	1.378(2)	N(11)–C(12)	1.459(2)
C(12)–C(13)	1.520(3)	C(13)–O(14)	1.410(2)
O(14)–C(15)	1.420(2)	C(15)–C(16)	1.494(3)
C(16)–O(17)	1.422(2)	O(17)–C(18)	1.411(2)
C(18)–C(19)	1.479(3)	C(19)–O(20)	1.423(2)
O(20)–C(21)	1.423(2)	C(21)–C(22)	1.519(3)
C(22)–N(23)	1.465(2)	N(23)–C(24)	1.381(2)
N(23)–C(31)	1.372(2)	C(24)–C(25)	1.396(2)
C(24)–C(29)	1.390(2)	C(25)–C(26)	1.380(3)
C(26)–C(27)	1.387(3)	C(27)–C(28)	1.380(3)
C(28)–C(29)	1.397(3)	C(29)–N(30)	1.399(2)
N(30)–C(31)	1.316(2)	C(31)–C(32)	1.492(2)

C(2)–O(1)–C(32)	113.3(1)	O(1)–C(2)–C(3)	113.7(1)
C(2)–C(3)–N(4)	124.0(2)	C(2)–C(3)–N(11)	122.5(1)
N(4)–C(3)–N(11)	113.4(1)	C(3)–N(4)–C(5)	104.9(1)
N(4)–C(5)–C(6)	130.6(2)	N(4)–C(5)–C(10)	109.7(1)
C(6)–C(5)–C(10)	119.7(2)	C(5)–C(6)–C(7)	118.7(2)
C(6)–C(7)–C(8)	121.2(2)	C(7)–C(8)–C(9)	121.5(2)
C(8)–C(9)–C(10)	116.7(2)	C(5)–C(10)–C(9)	122.2(1)
C(5)–C(10)–N(11)	105.8(1)	C(9)–C(10)–N(11)	132.0(1)
C(3)–N(11)–C(10)	106.2(1)	C(3)–N(11)–C(12)	127.7(1)
C(10)–N(11)–C(12)	126.1(1)	N(11)–C(12)–C(13)	112.5(1)
C(12)–C(13)–O(14)	110.0(1)	C(13)–O(14)–C(15)	111.9(1)
O(14)–C(15)–C(16)	110.1(1)	C(15)–C(16)–O(17)	114.2(2)
C(16)–O(17)–C(18)	114.8(1)	O(17)–C(18)–C(19)	111.2(2)
C(18)–C(19)–O(20)	110.4(2)	C(19)–O(20)–C(21)	112.3(1)
O(20)–C(21)–C(22)	114.2(1)	C(21)–C(22)–N(23)	111.9(1)
C(22)–N(23)–C(24)	124.9(1)	C(22)–N(23)–C(31)	128.3(1)
C(24)–N(23)–C(31)	106.4(1)	N(23)–C(24)–C(25)	131.6(2)
N(23)–C(24)–C(29)	105.6(1)	C(25)–C(24)–C(29)	122.7(2)
C(24)–C(25)–C(26)	116.3(2)	C(25)–C(26)–C(27)	121.8(2)
C(26)–C(27)–C(28)	121.5(2)	C(27)–C(28)–C(29)	117.9(2)
C(24)–C(29)–C(28)	119.6(2)	C(24)–C(29)–N(30)	110.2(1)
C(28)–C(29)–N(30)	130.2(2)	C(29)–N(30)–C(31)	104.4(1)
N(23)–C(31)–N(30)	113.3(1)	N(23)–C(31)–C(32)	122.0(2)
N(30)–C(31)–C(32)	124.7(2)	O(1)–C(32)–C(31)	111.0(1)

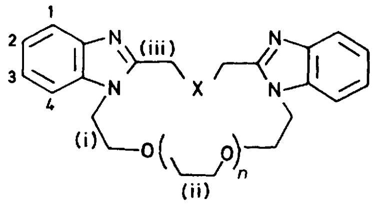

(A)

reflectance spectra were measured on the 550S instrument with an integrating sphere attachment. Visible spectra relating to the metal chromophores are in Table 6. N.m.r. spectra were taken on a Bruker FX90 or WB300 spectrometer. The data are in Table 7. Computer fitting of the spectra was done using the program NUMARIT.

Results and Discussion

The Ligands.—The new macrocycle L^7 was characterised by *X*-ray crystallography and the others by microanalysis and spectroscopic methods.

The n.m.r. studies of the open-chain ligands typically showed averaged spectra indicating two-fold symmetry on the n.m.r. time-scale. They typically had an AA′BB′ aromatic multiplet, indicating rapid exchange of the imidazole hydrogen between the two nitrogen sites {which was not quite at the fast-exchange limit for L^1 in [$^2H_6$]dimethyl sulphoxide, leaving the downfield aromatic multiplet [protons 1 and 4, see (**A**)] unresolved}, and a singlet for the aryl–CH_2 of L^1, L^2, L^3, and L^5. The OCH_2CH_2O segments were AA′BB′ systems with very small shift differences, but spectra taken at 300 MHz indicated values of *ca.* 8—10 Hz for *N*, the sum of the averaged vicinal couplings *J* and *J*′, consistent with the *gauche* form being the major conformation of these segments. The macrocycles essentially also had apparent two-fold symmetry, but their aromatic spectra were ABCD systems. The OCH_2CH_2O regions also had $N = ca.$ 9 Hz and apparent *gauche* segments, but the CH_2CH_2S segment of L^{10} was unusual. Complete analysis with NUMARIT gave values of $J = 10.6$ and $J' = 5.4$ (± 0.2) Hz indicative of a very high *trans* population distributed between the two averaged segments (iii), see (**A**). The open-chain compound L^4, from which L^{10} is derived, had a deceptively simple spectrum of two three-line multiplets, each line *ca.* 3 Hz wide, for the segment (iii), from which only the *N* value could be obtained ($N = 14$ Hz). This is also consistent with a high *trans* population for segment (iii). The corresponding n.m.r. spectrum of the open-chain oxygen analogue of L^4 was reported as a triplet with $J = 6.6$ Hz.[10] Thio analogues of crown ethers[22,23] have been reported to have conformations distinct from those of oxygen crowns, with SCH_2CH_2S torsion angles being *anti*, and the thioether usually exodentate to the ring, which has implications for the mechanism of reaction of the thio group with a metal

Table 4. Analytical data for metal complexes

Ligand	Formula of complex	M.p./°C	Colour	Analysis* (%)			
				C	H	N	S
L^1	$(C_{16}H_{14}N_4O)_2\cdot Cu(NO_3)_2\cdot EtOH$	249	Purple	51.1 (51.7)	4.0 (4.3)	17.4 (17.7)	
L^1	$C_{16}H_{14}N_4O\cdot AgNO_3$	285 (decomp.)	White	42.8 (42.9)	3.0 (3.1)	15.6 (15.6)	
L^2	$C_{18}H_{18}N_4O_2\cdot CuBr_2$	218	Olive	39.8 (39.6)	3.5 (3.3)	9.7 (10.3)	
L^2	$C_{18}H_{18}N_4O_2\cdot CuCl_2\cdot EtOH$	220	Light blue-green	47.5 (47.8)	4.6 (4.8)	11.1 (11.1)	
L^2	$C_{18}H_{18}N_4O_2\cdot Cu(NO_3)_2$	242	Blue-green	42.3 (42.4)	3.4 (3.5)	16.5 (16.5)	
L^2	$C_{18}H_{18}N_4O_2\cdot ZnCl_2\cdot 2H_2O$	320	White	43.5 (43.7)	4.1 (4.4)	11.3 (11.3)	
L^3	$C_{16}H_{14}N_4S\cdot CuBr_2$	200	Green	37.2 (37.1)	2.7 (2.7)	10.6 (10.8)	
L^3	$C_{16}H_{14}N_4S\cdot CuCl_2$	192	Blue-green	44.8 (44.8)	3.2 (3.3)	12.8 (13.1)	
L^3	$C_{16}H_{14}N_4S\cdot NiCl_2\cdot EtOH$	288	Green	45.5 (46.0)	4.1 (4.3)	11.9 (11.9)	
L^3	$C_{16}H_{14}N_4S\cdot ZnCl_2$	320	White	44.9 (44.6)	3.3 (3.3)	12.9 (13.0)	
L^3	$C_{16}H_{14}N_4S\cdot AgNO_3$	240	White	41.2 (41.4)	2.9 (3.0)	14.9 (15.1)	6.8 (6.9)
L^4	$C_{18}H_{18}N_4S\cdot Cu(NO_3)_2\cdot 2H_2O$	210	Blue	40.7 (40.5)	4.2 (3.8)	15.9 (15.9)	6.1 (5.9)
L^4	$C_{18}H_{18}N_4S\cdot Cu(SCN)_2$	182	Green	47.9 (47.9)	3.6 (3.6)	17.2 (16.7)	18.9 (19.1)
L^5	$C_{22}H_{18}N_4O_2\cdot CuBr_2$	235	Dark green	44.5 (44.5)	3.0 (3.1)	9.3 (9.4)	
L^5	$C_{22}H_{18}N_4O_2\cdot CuCl_2\cdot H_2O$	237	Blue	50.6 (50.5)	3.5 (3.9)	10.5 (10.7)	
L^5	$C_{22}H_{18}N_4O_2\cdot NiBr_2\cdot EtOH$	250	Orange	46.8 (45.4)	3.8 (3.8)	9.1 (8.8)	
L^5	$C_{22}H_{18}N_4O_2\cdot NiCl_2\cdot 3H_2O$	265	Orange	47.7 (47.8)	4.4 (4.4)	10.2 (10.1)	
L^5	$C_{22}H_{18}N_4O_2\cdot ZnCl_2\cdot EtOH$	288	White	51.4 (52.2)	4.1 (4.4)	10.0 (10.1)	
L^5	$(C_{22}H_{18}N_4O_2)_2\cdot Cu_3(SCN)_6$	205	Green	47.1 (46.9)	2.7 (2.8)	14.8 (15.3)	
L^7	$C_{24}H_{28}N_4O_4\cdot CuBr_2$	204	Yellow	43.0 (43.7)	4.1 (4.2)	7.9 (8.5)	
L^8	$C_{26}H_{24}N_4O_3\cdot CuBr_2$	205	Brown	46.4 (47.0)	3.5 (3.6)	8.2 (8.4)	
L^8	$C_{26}H_{24}N_4O_3\cdot CuCl_2$	218	Green	52.4 (54.3)	3.8 (4.2)	10.1 (9.7)	
L^8	$C_{26}H_{24}N_4O_3\cdot ZnCl_2$	290	White	52.0 (54.1)	4.0 (4.2)	9.7 (9.7)	
L^{11}	$C_{24}H_{28}N_4O_2S\cdot Cu(NO_3)_2$	208	Blue	45.7 (46.5)	4.7 (4.5)	12.4 (13.4)	5.4 (5.1)
L^{11}	$C_{24}H_{28}N_4O_2S\cdot CuBr_2\cdot H_2O$	165	Yellow	42.0 (42.5)	4.5 (4.4)	7.7 (8.3)	5.1 (4.7)

* Required values in parentheses.

ion.[22,23] The situation for L^{10} would seem to favour co-ordination of copper *exo* to the macrocycle, only after reorganisation to a *gauche* form.

The crystal structure of the 18-membered crown macrocycle L^7 revealed an interesting contrast to other 18-membered ring crown macrocycles which have been analysed by *X*-ray techniques.[24] Atomic co-ordinates for the non-hydrogen atoms are given in Table 2. The view in Figure 2 is taken to show the parallel but stepped locations of the benzimidazole rings adopted in this unusual ligand. The numbering scheme for the atoms is shown in Figure 3. The bond lengths and angles of the structure fall within the expected ranges. The tendency of benzimidazoles to stack in complexes of this type of ligand has been noted previously.[12] This provides a major constraint on the conformation of L^7 but remarkably, the oxygens of the polyether chain retain the *gauche* relation common for unstrained crown ethers. This may be verified from Figure 2, in which the torsion angles of the macrocyclic ether ring of L^7 are shown [*cf.* those for 18-crown-6 (1,4,7,10,13,16-hexaoxacyclooctadecane) and its analogues[24]].

Metal(II) *Complexes*.—Solid complexes of the ligands with various salts of Cu^{II}, Ni^{II}, and Zn^{II} were prepared and generally a 1:1 L:M ratio was found. A pure sample of a 2:1 L:Cu complex of L^1 could be obtained from solutions containing a ratio of L:M higher than 2:1.

U.V. and Visible Spectra.—The investigation of u.v. and visible spectra was directed to determining the number and nature of species in solution for copper complexes of ligands L^1—L^5, comparison of solid-state reflectance and solution spectra for a number of complexes, consideration of charge-transfer bands in the near-u.v., and comparison of the NON and NOON ligands with their NSN and NSSN analogues. In the u.v. absorption spectra of the ligands, the bands at *ca.* 270 and *ca.* 240—255 nm were composite. The band at *ca.* 270 nm usually had a high frequency shoulder, which was more pronounced in the macrocyclic compounds, and which resolved into two separate maxima for the macrocycle L^9. The band at *ca.* 240—255 nm (which had at least one shoulder) was most sensitive to the nature of the metal. In the macrocycles, the band was at *ca.* 255 nm and had a shoulder at higher frequencies, *ca.* 248 nm. In the copper(II) complexes, the intensities of the two components were reversed, the shoulder now being on the low frequency side of the main band. In the open-chain ligands, this band was at *ca.* 240 nm and had a low frequency shoulder, retained in the copper complexes *e.g.* of L^4. In the visible region, the spectrum of solvated copper ions was shifted to higher frequencies on complexation; new bands of low intensity ($\varepsilon \sim 200$ dm^3 mol^{-1} cm^{-1}) may be assigned as ligand-field bands, while more intense bands in the near-u.v. (ε *ca.* 400—4 000 dm^3 mol^{-1} cm^{-1}) are probably charge-transfer bands.[11] The data are shown in Table 6. The colours of the copper complexes varied from blue, through olive, to yellow-brown, depending on the relative influence of the blue copper ligand-field band in the near i.r., and the tail of the charge-transfer interaction in the near-u.v. The Job's Plot method (applied to the visible spectrum only) indicated that 1:1 complexes were the major species stable in dimethyl sulphoxide solutions of ligands L^2, L^3, and L^5 with Cu^{II} salts and in ethanol solutions of all except L^1.

For L^1 both 1:1 and 2:1 L:M complexes were observed with the Job's Plot method and the purple solution indicated a new

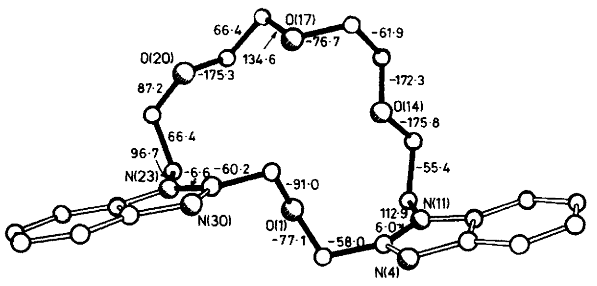

Figure 2. Torsion angles (°) in the macrocyclic ring of L^7

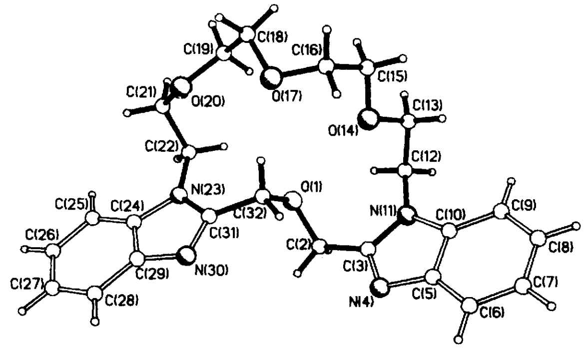

Figure 3. The numbering scheme for the atoms of L^7

Table 5. U.v. absorption spectra of free ligands * and metal complexes

Ligand	Salt	$\lambda_{max.}$/nm (ε/dm^3 mol^{-1} cm^{-1})			
L^1		281 (12 200)	273 (14 500)	245 (12 700)	
L^1	$CuBr_2$	278 (17 600)	271 (17 000)	238 (15 130)	
L^2		278 (12 500)	271 (14 900)	243 (13 700)	
L^2	$CuBr_2$	279 (19 000)	272 (19 200)	246 (sh) (15 800)	
L^2	$ZnCl_2$	278 (14 400)	272 (17 400)	245 (14 200)	
L^3		285 (20 100)	278 (19 500)	246 (14 200)	
L^4		278 (17 400)	273 (17 000)	241 (sh) (14 000)	
L^4	$CuBr_2$	275 (16 200)	268 (16 500)	239 (12 600)	
L^5		280 (17 000)	273 (20 200)	245 (16 100)	
L^5	$CuBr_2$	276 (22 000)	270 (21 300)	240br (13 900)	
L^6		282 (12 000)	275 (14 200)	252 (15 000)	
L^6	$CuBr_2$	280 (14 400)	272 (15 400)	245 (15 000)	
L^6	$ZnCl_2$	278 (13 400)	271 (14 000)	250 (13 800)	
L^7		283 (10 200)	275 (12 000)	252 (13 500)	
L^7	$CuBr_2$	278 (15 600)	271 (15 400)	254 (15 400)	
L^7	$ZnCl_2$	278 (14 400)	272 (13 200)	250 (13 200)	
L^8		280 (19 200)	274 (22 400)	250 (14 200)	
L^8	$CuBr_2$	278 (22 400)	271 (23 200)	250 (19 000)	
L^9		284 (13 500)	276 (15 000)	254 (19 500)	268 (14 000)
L^9	$Cu(NO_3)_2$	281 (15 000)	272 (15 600)	247 (15 000)	265 (12 900)
L^9	NaI	284 (13 400)	276 (15 400)	254 (19 000)	268 (13 800)
L^{10}		283 (15 900)	275 (15 600)	253 (15 500)	
L^{10}	$Cu(NO_3)_2$	281 (15 700)	273 (16 500)	247, 253 (14 500)	
L^{11}		283 (17 130)	276 (17 350)	253 (18 450)	
L^{11}	$Cu(NO_3)_2$	281 (15 900)	273 (17 640)	254 (13 380)	
L^{11a}		283 (14 700)	276 (14 700)	253 (sh) (15 360)	
L^{11a}	$Cu(NO_3)_2$	280 (14 280)	273 (15 000)	247 (sh) (12 840)	

* Solutions in ethanol.

Table 6. U.v. and visible spectra of metal complexes (1:1 L:M unless otherwise stated)

Ligand	Salt	Frequencies[a] (10^3 cm^{-1})				
L^1	$CuCl_2$[b]	33.0	29.0	24.75		12.0
L^3	$CuCl_2$[b,c]		27.0		15.9s	12.7w
L^1	$CuBr_2$[d]	32.4 (1 800)	26.3 (430)		15.0—14.0 (140)	
L^3	$CuBr_2$[b,c]		29.5	25.0	15.9—15.4	12.2
L^1	$Cu(NO_3)_2$[b,e]		29.0vs		18.2vs	14.0—13.0
f	$Cu(ClO_4)_2$[b,e]			26.7	20.0	14.7
f	$Cu(ClO_4)_2$[d,e]			27.8	18.2	15.0
L^2	$CuBr_2$[b]		29.2vs	24.6	21.8	14.5—15.0br
L^2	$CuBr_2$[d]	32.7 (3 500)	27.8 (1 190)		15.0 (150)	
g	$CuBr_2$[d]				15.0 (550)	11.3 (260)
g	$CuCl_2$[b]				14.9w	11.2s
L^2	$Cu(NO_3)_2$[b]		29.2	25.4	15.4—15.0	
L^5	$CuBr_2$[b]		28.6	24.5	14.3	
L^5	$CuBr_2$[d]	33.0 (3 030)	27.9 (1 380)		15.8—15.4 (180)	
h	$Cu(ClO_4)_2$[b]				15.9w	11.8s
h	$Cu(ClO_4)_2$[d]				14.5 (120)	

[a] Absorption coefficients (dm^3 mol^{-1} cm^{-1}) in parentheses. [b] Solid-state reflectance. [c] Thio analogue of L^1. [d] In ethanol. [e] 2:1 Complex. [f] NSN Ligand, ref. 11. [g] NSSN Ligand, ref. 7. [h] NSSN ligand, ref. 8.

Table 7. N.m.r. absorptions of free and complexed ligands [proton numbering as in (**A**)]

Ligand	Aromatics	SCH_2 (iii)	Aryl–CH_2 (iii)	NCH_2 (i)	OCH_2 (i)	OCH_2 (ii)	Solvent/salt
L^6	7.87, 7.33		5.13 (s)	3.75	4.45	3.25	*a*
L^7	7.62, 7.27		5.067 (s)	3.694	4.556	3.356	*b*
L^7	7.62, 7.24		5.04 (s)	3.69	4.55	3.33	*b*, *c*
L^9	7.63, 7.52 7.29, 7.26		4.91 (s)	3.807	4.477	3.39 3.34	*d*, *e*
L^9	7.61, 7.56 7.30		4.95 (s)	3.80	4.499	3.41 3.35	*c*, *d*, *f*
L^{10}	7.52, 7.17	3.308	3.236	3.694	4.376	3.40	*b*
L^{10}		3.305	3.208	3.771	4.322	3.40	*a*, *g*
L^1	7.56, 7.18		4.868 (s)				*b*
L^1	7.92, 7.32		4.98 (s)				*b*, *h*
L^1	7.38, 7.07		5.199 (s)				*b*, *i*
L^4	7.63, 7.326	3.386	3.087				*a*, *j*

[a] $CDCl_3$. [b] 0.1 mol dm^{-3} [$^2H_6$]dimethyl sulphoxide. [c] Also 0.1 mol dm^{-3} in KSCN. [d] 0.1 mol dm^{-3} in CD_3OD. [e] N = 10.7 (i), 8.0 Hz (ii). [f] N = 10.47 (i), 7.89 Hz (ii). [g] N = 16.0 Hz (iii). [h] Also 0.1 mol dm^{-3} in $ZnCl_2$. [i] Also 0.1 mol dm^{-3} in $AgNO_3$. [j] N = 13.95 Hz (iii).

complex at the 2:1 composition. The purple 2:1 complex of L^1 has a visible spectrum similar to that of the orange-brown 2:1 complex of Cu^{II} with a ligand[11] containing NSN donor groups, whose octahedral co-ordination (found also for the 2:1 complex in ref. 4) is shown in Figure 1(*d*). Our purple complex was probably of the same geometry, with a square-planar array of four N, and two weak axial interactions. Since the solution and reflectance spectra of this purple complex correspond, the structure is probably preserved in solution.

A comparison of the 1:1 complexes of the ligands L^2—L^5 and their S or O analogues is possible. In each case a crystal structure of a complex of the thio ligand is available, together with a solid-state u.v.–visible spectrum. If the geometry of each complex is conserved on replacement of S by O co-ordination, this should be detected in slight red shifts of the ligand-field absorption bands. The complexes of L^1 and L^3 are dissimilar; the substantial red shift is much greater than expected and more probably represents a change in geometry. While the spectra of L^2 are similar in the solid and solution, and resemble the solution spectra of the thio analogue, these all differ from the solid-state spectrum of the thio analogue whose trigonal bipyramidal structure is known. The same observations may be made for L^5, and its thio analogue.[8] The complexes of ligands L^2 and L^5 are thus not trigonal bipyramidal in the solid and solution, but are probably distorted octahedral.

Some solution n.m.r. studies were carried out. Considerable shifts in the ^1H n.m.r. spectrum of ligands in the presence of equimolar amounts of metal salts in [$^2H_6$]dimethyl sulphoxide indicated complex formation, as has been noted in earlier work.[5] Results are in Table 7. The zinc chloride interaction with L^1 gave very considerable shifts of the two downfield aromatic protons [1 and 4, see (**A**)] suggesting asymmetric co-ordination of zinc to one nitrogen of each benzimidazole. The downfield multiplet [hydrogens 1 and 4, see (**A**)] was very poorly resolved, indicating an averaging system not yet at the fast-exchange limit. The upfield multiplet was sharply resolved. However, for the $AgNO_3$ interaction with L^1, the protons of the bridge are more strongly affected than the aromatics, which are also very sharply resolved (better than in the free ligand). The silver must have a different co-ordination mode.

For macrocycles with ether donors, we hoped to find an alkali-co-ordinating function. The ligand L^7 was examined in solution with KSCN, and no discernible change in the proton spectrum was found. Moreover, the more sensitive ^{23}Na n.m.r. technique was tried with a methanol solution 0.1 mol dm^{-3} in NaI and 0.025, 0.05, and 0.1 mol dm^{-3} in L^9. The linewidths of the relevant single-line sodium resonances were 17.5, 22.0, and 25.0 Hz. The ^{1}H n.m.r. spectrum (at 300 MHz) of this ligand was examined in the presence and absence of a two-fold excess of NaI. The maximum shift of any proton was 10 Hz, and the least 1 Hz downfield, and there were slight changes in the coupling constants. The detailed analysis of the data is in Table 7. This indicates the interaction with alkali cations is slight.

We were also unable to demonstrate any transport of sodium or potassium picrate in the presence of the macrocycle L^6, nor could we find any evidence of interaction in u.v. studies of the ligand absorbances in the presence of alkali-metal salts.

Acknowledgements

We thank the S.E.R.C. for financial support, Miss Audrey Tate and Miss Dawn Carus for some preliminary work, and Mrs. L. Cook for experimental assistance.

References

1 E. I. Solomon, K. W. Penfield, and D. E. Wilcox, *Struct. Bonding (Berlin)*, 1983, **53**, 1.

2 'Copper Proteins,' ed. T. G. Spiro, Wiley, New York, 1981.

3 E. T. Adman and L. H. Jensen, *Isr. J. Chem.*, 1981, **21**, 8.

4 H. P. Berends and D. W. Stephan, *Inorg. Chim. Acta*, 1984, **93**, 173.

5 M. J. Schilstra, P. J. M. W. L. Birker, G. C. Verschoor, and J. Reedijk, *Inorg. Chem.*, 1982, **21**, 2637.

6 P. J. M. W. L. Birker, E. F. Godefroi, J. Helder, and J. Reedijk, *J. Am. Chem. Soc.*, 1982, **104**, 7556.

7 P. J. M. W. L. Birker, J. Helder, G. Henkel, B. Krebs, and J. Reedijk, *Inorg. Chem.*, 1982, **21**, 357.

8 F. J. Rietmeijer, P. J. M. W. L. Birker, S. Gorter, and J. Reedijk, *J. Chem. Soc., Dalton Trans.*, 1982, 1191.

9 J. van Rijn, W. L. Driessen, J. Reedijk, and J-M. Lehn, *Inorg. Chem.*, 1984, **23**, 3584.

10 A. W. Addison, P. J. Burke, K. Henrick, T. N. Rao, and E. Sinn, *Inorg. Chem.*, 1983, **22**, 3645.

11 H. J. Prochaska, W. F. Schwindiger, M. Schwartz, M. J. Burk, E. R. Bernarducci, R. A. Lalancette, J. A. Potenza, and H. J. Schugar, *J. Am. Chem. Soc.*, 1981, **103**, 3446.

12 K. Takahashi, Y. Nishida, and S. Kida, *Polyhedron*, 1984, **3**, 113.

13 A. W. Addison, H. M. J. Hendriks, J. Reedijk, and L. K. Thompson, *Inorg. Chem.*, 1981, **20**, 103.

14 J. V. Dagdigian and C. A. Reed, *Inorg. Chem.*, 1979, **18**, 1979.

15 D. E. Wilcox, J. R. Long, and E. I. Solomon, *J. Am. Chem. Soc.*, 1984, **106**, 2186.

16 M. A. Phillips, *J. Chem. Soc.*, 1928, 2393.

17 P. N. Preston, *Chem. Rev.*, 1974, **74**, 279.

18 W. Clegg, *Acta Crystallogr., Sect. A*, 1981, **37**, 22.

19 G. M. Sheldrick, SHELXTL, an integrated system for solving, refining and displaying crystal structures from diffraction data, University of Göttingen, 1978.

20 D. Rogers, *Acta Crystallogr., Sect. A*, 1981, **37**, 734.

21 'International Tables for *X*-Ray Crystallography,' Kynoch Press, Birmingham, 1974, vol. 4, pp. 99, 149.

22 W. N. Setzer, C. A. Ogle, G. S. Wilson, and R. S. Glass, *Inorg. Chem.*, 1983, **22**, 266 and refs. therein.

23 J. R. Hartman, R. E. Wolf, B. M. Foxman, and S. R. Cooper, *J. Am. Chem. Soc.*, 1983, **105**, 131.

24 M. Dobler, 'Ionophores and Their Structures,' John Wiley and Sons, New York, 1981.

Received 25th February 1985; *Paper* 5/314